

Correlation of NASA Low-Speed Compressor Test Results with AeroDynamic Solutions, Inc. CFD Code

NOTE TO READER

Attached is an analysis completed in February 2010 by a commercial aircraft engine company comparing laser anemometer data from a NASA low-speed centrifugal compressor against CFD predictions from Code Leo.

The analysis focuses primarily on predictive accuracy. Though it has not received “formal” case study treatment, we felt it would be valuable to post to our website for you to see in its original, unedited form.

At the evaluator’s request, we have removed the name of the author and company from the document.

A few comments:

- *Source data.* The original report, *Laser Anemometer Measurements of the Three-Dimensional Rotor Flow Field in the NASA Low-Speed Centrifugal Compressor*, was published by Hathaway et al in July 1995. This report may be found on the NASA Technical Report Server. Click [here](#) to view the report abstract.
- *Uncertainty.* Uncertainty in experimental data measurements, as specified in the original NASA report, were as follows:
 - Individual velocity component measurements : +/- 1.5 m/s
 - Measured velocity components : <2° of the throughflow component, except in regions of high unsteadiness
 - Laser anemometer readings: +/- 2° for pitch angle
- *Turnaround time.* According to the author, a “couple of hours” of setup time was required generate the mesh with Code Wand. Code Leo required ~8,000 iterations to converge to a solution (2 hours, 21 minutes on a single CPU running 32-bit Linux).

**Correlation of NASA Low-Speed Compressor
Test Results with AeroDynamic Solutions, inc.
CFD Code.**

February 3, 2010

Reported by [REDACTED]

[REDACTED]

Contents

List of Figures.....	2
A. Introduction.....	3
B. Rotor Geometry.....	3
C. Available Test Data.....	4
D. CFD Boundary Conditions Defined.....	4
E. CFD Mesh Details.....	8
F. Available Test Data.....	10
G. References.....	16

List of Figures

Figure 1, Test Rig Flowpath.....	5
Figure 2, CFD Flowpath.....	6
Figure 3, Inlet Mach Number Profile.....	7
Figure 4, Inlet Mach Number Profile.....	7
Figure 5, Inlet Swirl Angle Profile.....	8
Figure 6, Inlet Pitch Angle Profile.....	8
Figure 7, Rotor Blade LE Mesh.....	9
Figure 8, Rotor Blade TE Mesh.....	10
Figure 9, Rotor Total Pressure Ratio vs. Flow.....	11
Figure 10, Normalized Total Temperature Rise vs. Flow.....	12
Figure 11, Rotor Efficiency vs. Flow.....	12
Figure 12, Rotor Total Pressure Ratio vs. Flow.....	13
Figure 13, Rotor Total Pressure Ratio vs. Flow.....	14
Figure 14, Blade-Blade Tangential Velocity Profile, Rotor Exit, 20% Span from Hub... 15	15
Figure 15, Blade-Blade Tangential Velocity Profile, Rotor Exit, 50% Span from Hub... 15	15
Figure 16, Blade-Blade Tangential Velocity Profile, Rotor Exit, 80% Span from Hub... 16	16

A. Introduction

The NASA low-speed compressor (LSC) is a relatively large centrifugal compressor, constructed in order to facilitate taking detailed flow measurements within an operating centrifugal compressor. The test data and compressor geometry are available to the public, and were used as a CFD test case for ADS CFD.

The test rig consisted of a centrifugal compressor driven by an electric motor, with a long vaneless diffuser and volute collector downstream. The compressor was fed through a bellmouth equipped with a bank of air straighteners to ensure uniform, swirl-free inlet conditions.

Laser anemometer data were recorded through the rotor and into the vaneless diffuser. Probe traverses were performed at the compressor inlet and exit. In addition, the compressor blades were instrumented with dozens of static pressure taps using piezoelectric pressure transducers to measure the blade loadings.

B. Rotor Geometry

- Design tip speed: 502 ft/s (1862 RPM)
- Design mass flow: 66 lbm/s
- 20 full blades, no splitters
- Exit backsweep: 55 degrees
- Inlet diameter: 3.281 ft
- Inlet blade height: 0.715 ft.
- Exit diameter: 5 ft.
- Exit b-width: 0.463 ft.
- Tip Clearance: .100", .100", .100" (LE, mid-chord, TE)

The compressor blade geometry was provided in the form of cylindrical coordinate data files, which were used as geometry input to code WAND. The meridional flowpath was defined by a Cartesian coordinate file.

The low speed of the compressor and the small pressure ratio imply that the rotor geometry is not subject to significant thermal or centrifugal loads that typically deform compressor rotors. This fact lends confidence to the similarity of the geometry modeled to the actual hardware geometry during operation.

Technical drawings of the rotor were not provided.

C. Available Test Data

- Rotor inlet and exit traverses
 - P_o, P_s, T_o , flow angles
- Laser anemometer surveys
 - Axisymmetric surfaces of revolution, ~normal to shroud at 20 locations
 - Axial, radial, relative tangential velocity components
 - Flank milled design allowed measurements very close to blade surfaces
- Static pressure taps
 - Shroud flow path
 - Blade surfaces resolved both in span and meridional direction (9 “chord-wise measurement lines”)

D. CFD Boundary Conditions Defined

- Inlet
 - Air angle profiles specified (pitch and yaw)
 - Total pressure profile specified
 - Mach number profile specified
 - Inlet temperature profile not specified – 518.67 constant used
- Exit
 - Static pressure adjusted to meet mass flow.
- Detailed flow path and rotor geometry provided
- Adiabatic wall assumed

Figure 1 is a meridional view of the test rig flowpath. The wedge shapes in the vaneless diffuser were added to eliminate flow separation at the walls.

The geometry of the vaneless diffuser was smoothed for CFD modeling, and is shown in Figure 2.

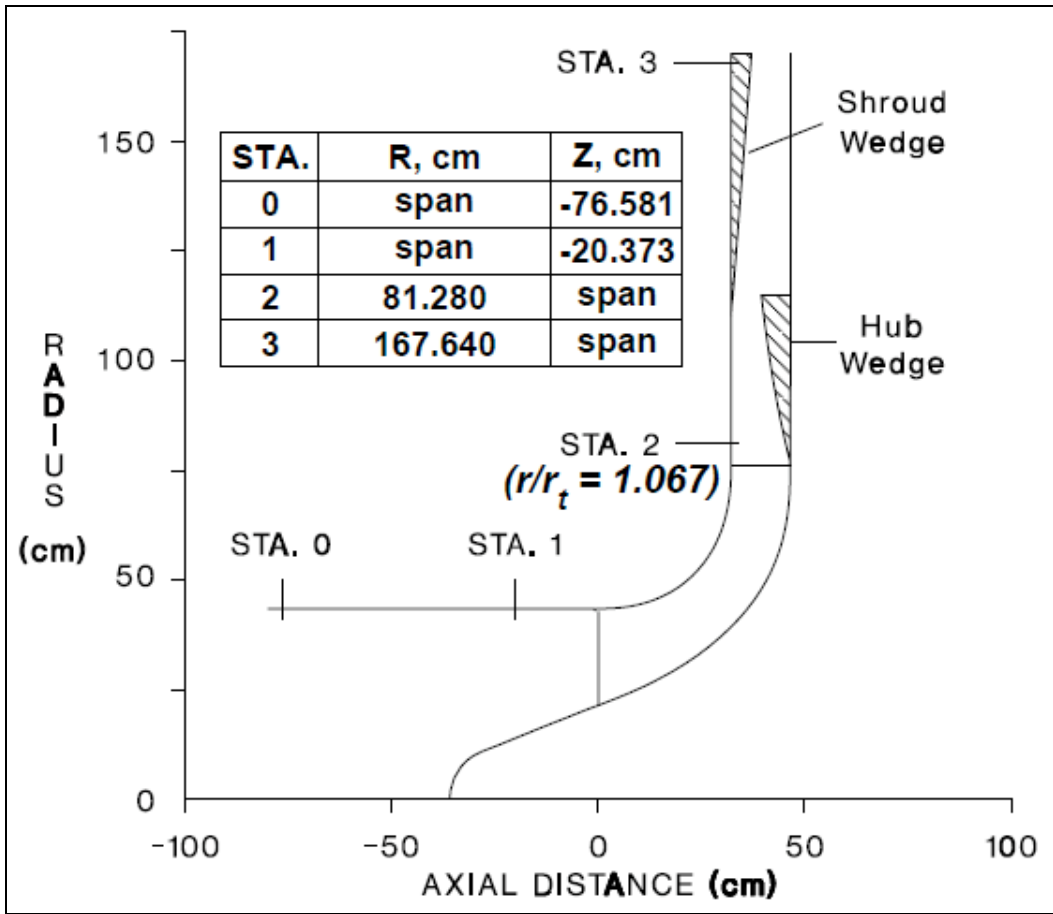


Figure 1, Test Rig Flowpath¹

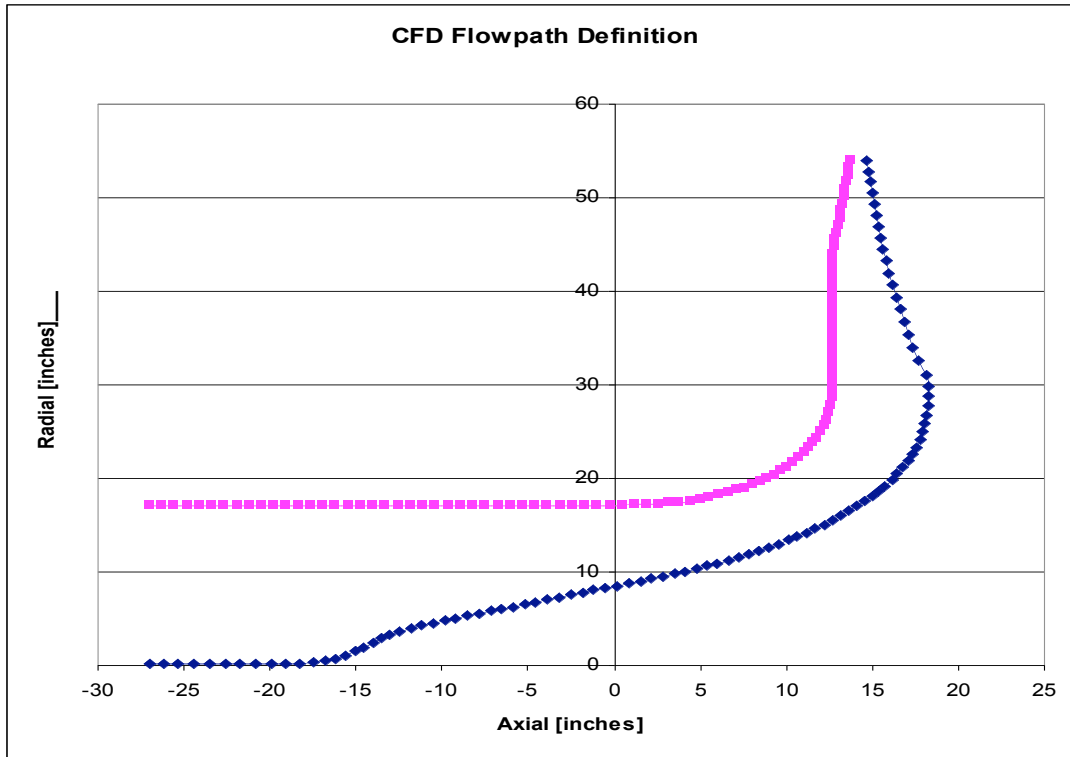


Figure 2, CFD Flowpath

Inlet traverses were performed during rig operation, and these data were used to specify CFD inlet aerodynamic boundary conditions.

Figures 3 and 4 compare the measured Mach number and total pressure profiles, respectively, to the specified distribution in the CFD case. The CFD boundary conditions appear to resolve the measured profiles adequately.

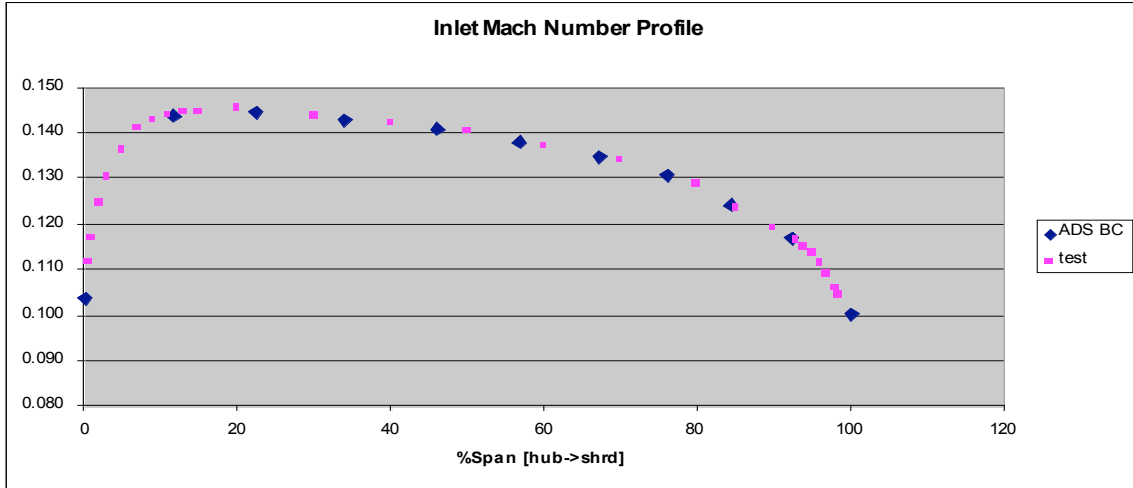


Figure 3, Inlet Mach Number Profile

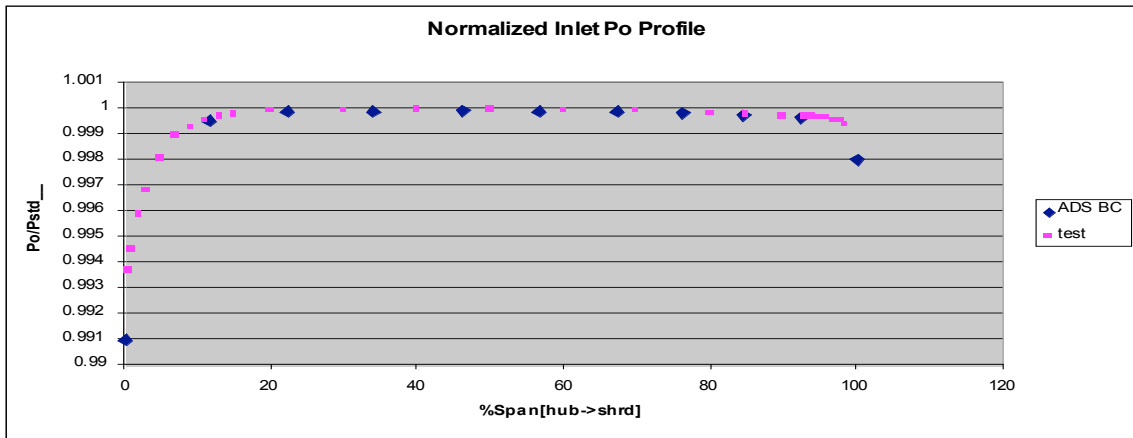


Figure 4, Inlet Mach Number Profile

Figures 5 and 6 compare the measured swirl angle and pitch angle profiles, respectively, to the specified distribution in the CFD case. Again, the CFD boundary conditions appear to resolve the measured profile adequately.

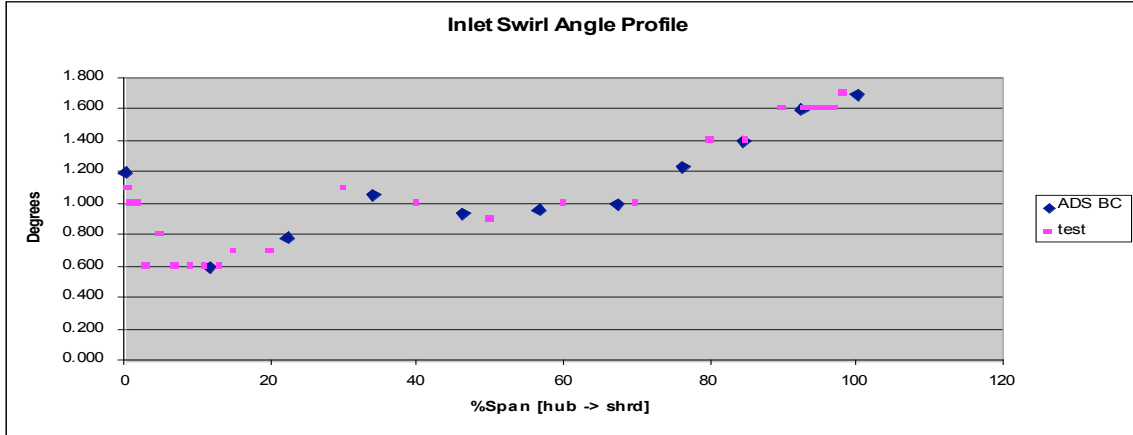


Figure 5, Inlet Swirl Angle Profile

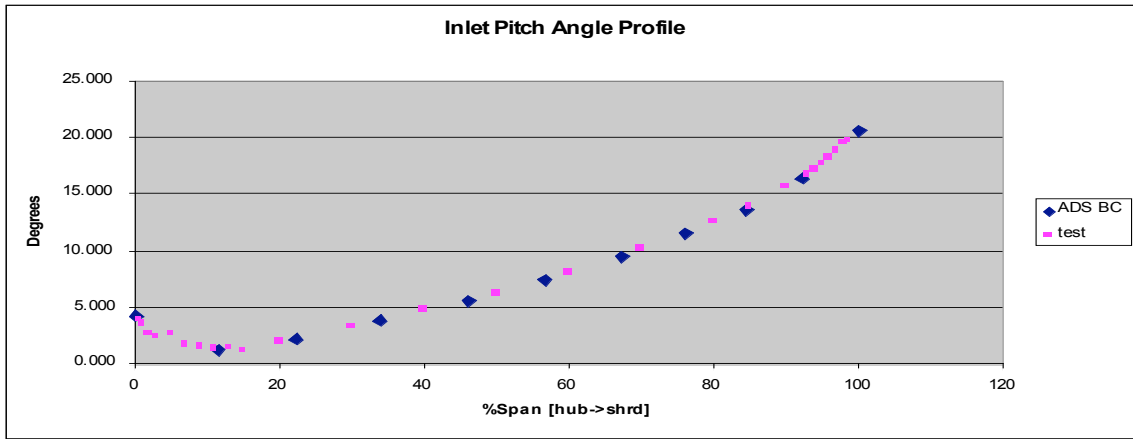


Figure 6, Inlet Pitch Angle Profile

Inlet profiles were provided by NASA for only two operating conditions: the design flow and RPM (66.2 lbm/s, 1862 RPM), and one off-design condition (52.1 lbm/s, 1862 RPM). The inlet conditions for the two cases were nearly identical, so the above profiles were used for all flow conditions simulated in ADS.

E. CFD Mesh Details

- Node count: 229466
- Structured hex mesh

The CFD mesh was generated with code WAND. The mesh generation was very simple and rapid, requiring essentially no extra “tweaking” beyond setting up WAND input files.

Wall y^+ values were generally between 0.2 and 1.0, which is generally satisfactory for turbulence modeling.

Note that a mesh independence study was not performed during this evaluation.

The figures below are mid-span mesh images at the leading and trailing edges of the rotor blades. All blade edges appear to be well resolved. There are some relatively large “jumps” in axial length of some of the cells near the leading edge, as well as some skewing of the cells in the vicinity of the jumps.

The trailing edge mesh looks very nice.

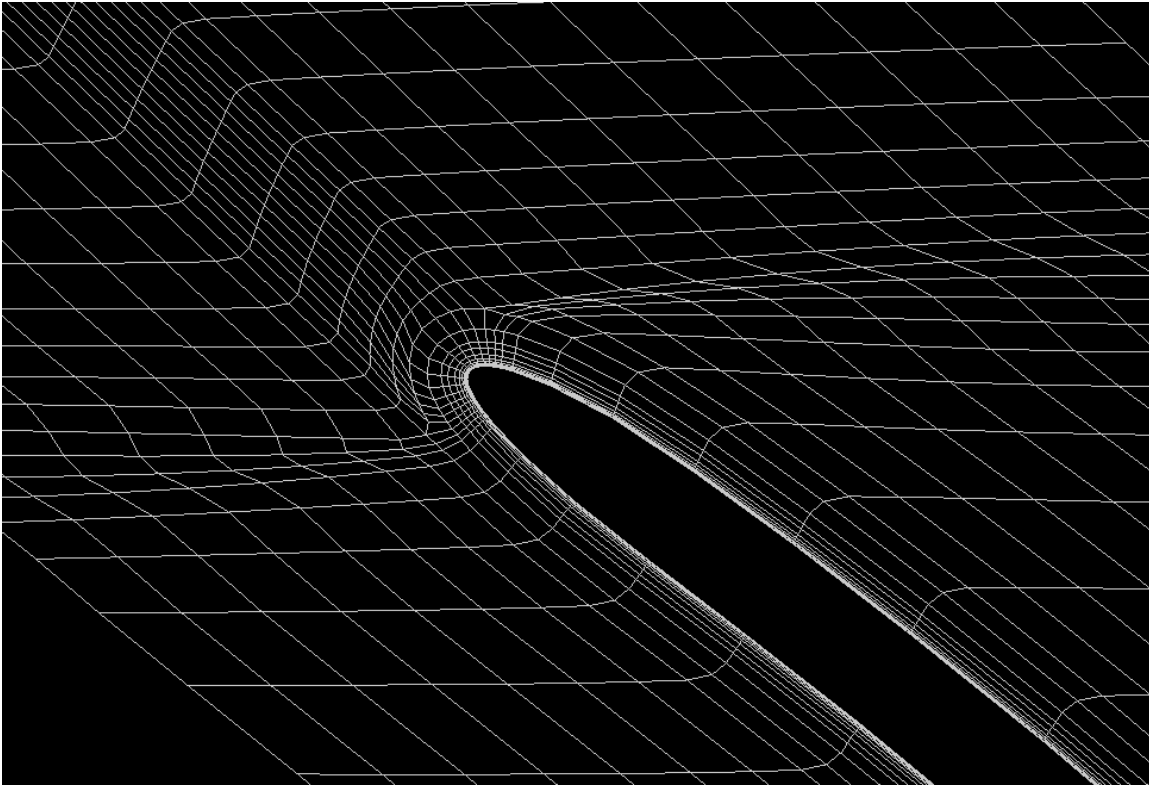


Figure 7, Rotor Blade LE Mesh

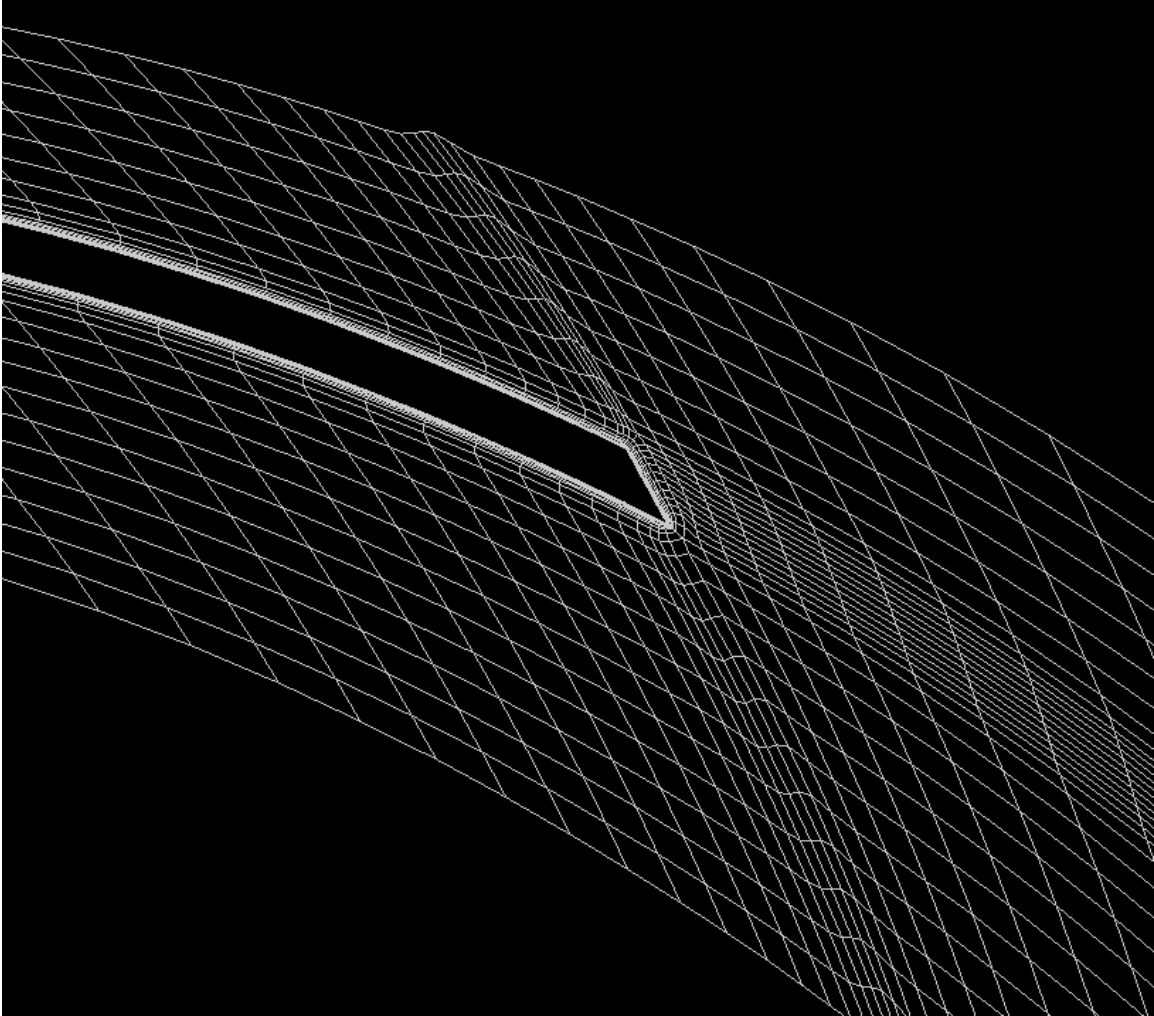


Figure 8, Rotor Blade TE Mesh

F. Available Test Data

The test rotor exit traverse was performed 2.0" downstream of the rotor exit ($R=32''$), at a radius ratio of 1.067. Total pressure was computed by an "energy averaging" scheme, outlined in the NASA report. In brief, they're mass averaging enthalpy ratio and converting to a pressure ratio. The equation below is the method used for this averaging:

$$\frac{\overline{P_0}}{P_{0_inlet}} = \left[\frac{\sum \left[\left(\frac{P_{o,i}}{P_{0_inlet}} \right)^{\frac{\gamma-1}{\gamma}} \rho_i (V_{radial})_i (\Delta A)_i \right]}{\sum [\rho_i (V_{radial})_i (\Delta A)_i]} \right]^{\frac{\gamma}{\gamma-1}}$$

This “i” subscript refers to the span-wise incremental measurement, where the subscript increases from hub to shroud.

The computed total pressure ratio across the rotor reported from CFD is the mass-averaged value at R= 32”.

Figures 9-11 show excellent agreement between performance computed using CFD and test measurements.

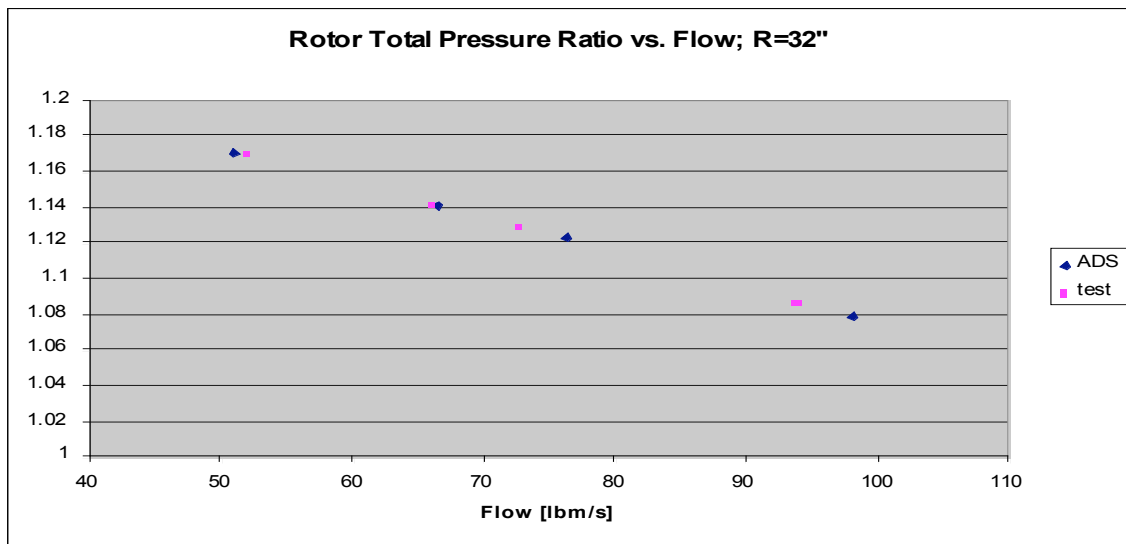


Figure 9, Rotor Total Pressure Ratio vs. Flow

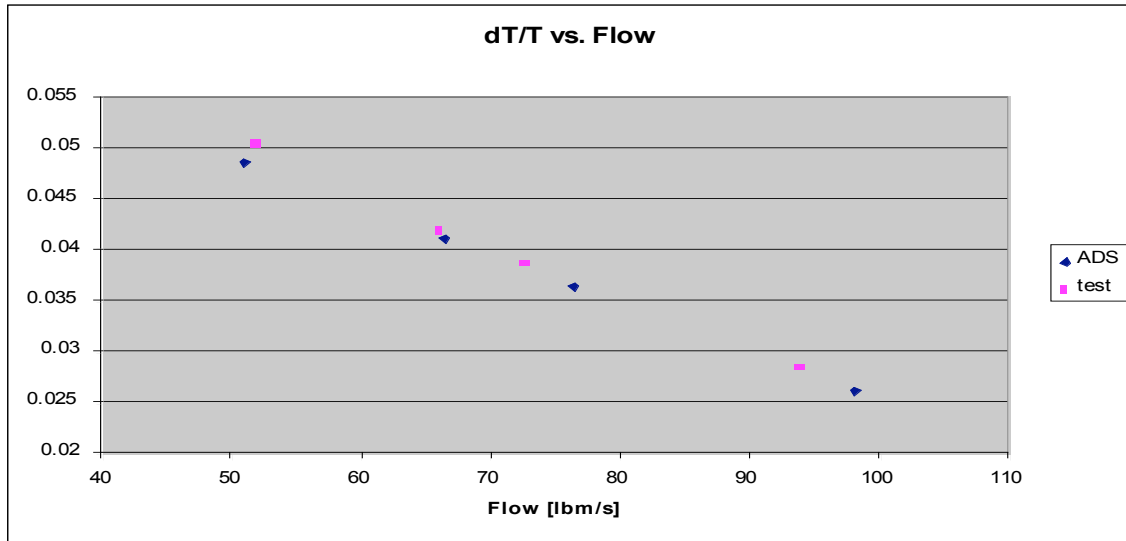


Figure 10, Normalized Total Temperature Rise vs. Flow

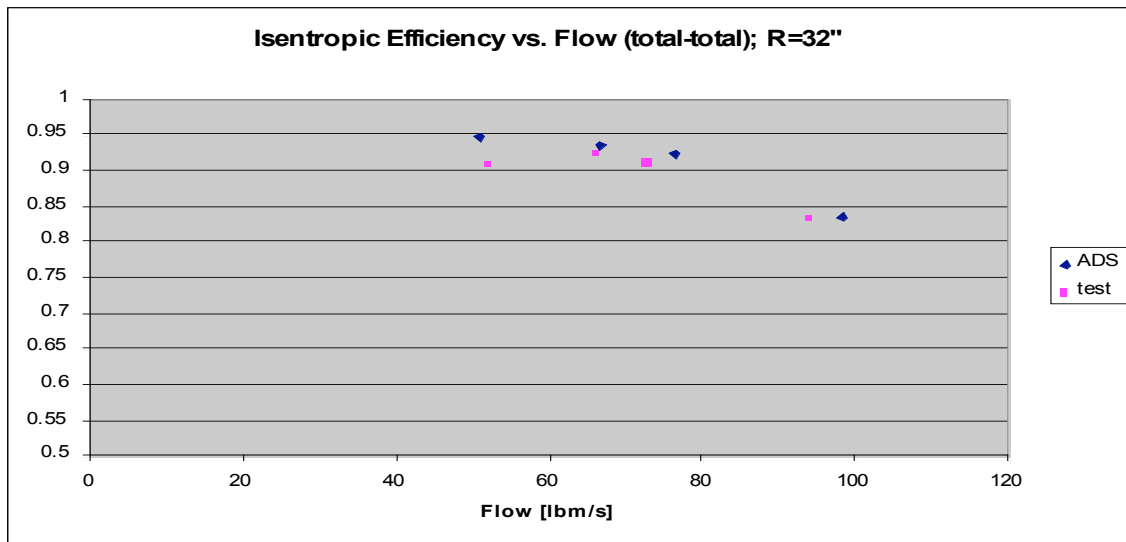


Figure 11, Rotor Efficiency vs. Flow

Note that the measured values of total pressure ratio and dT/T align almost perfectly with CFD, but that there is a noticeable difference in the efficiency plot. This is likely due to variation in the methods (and assumptions) used to compute efficiency.

Figures 12 and 13 compare calculated and measured rotor exit flow angles and total pressure profiles, respectively. The design point was used for this comparison.

Note that the greatest discrepancy between CFD and test occurs near the walls for both measurements. It is quite possible that some of these differences are due to probe inaccuracies near the wall, and that the CFD yields a more accurate result than test. However, the laser anemometer measurements presented below are not subject to these wall effects, and yet a similar trend persists.

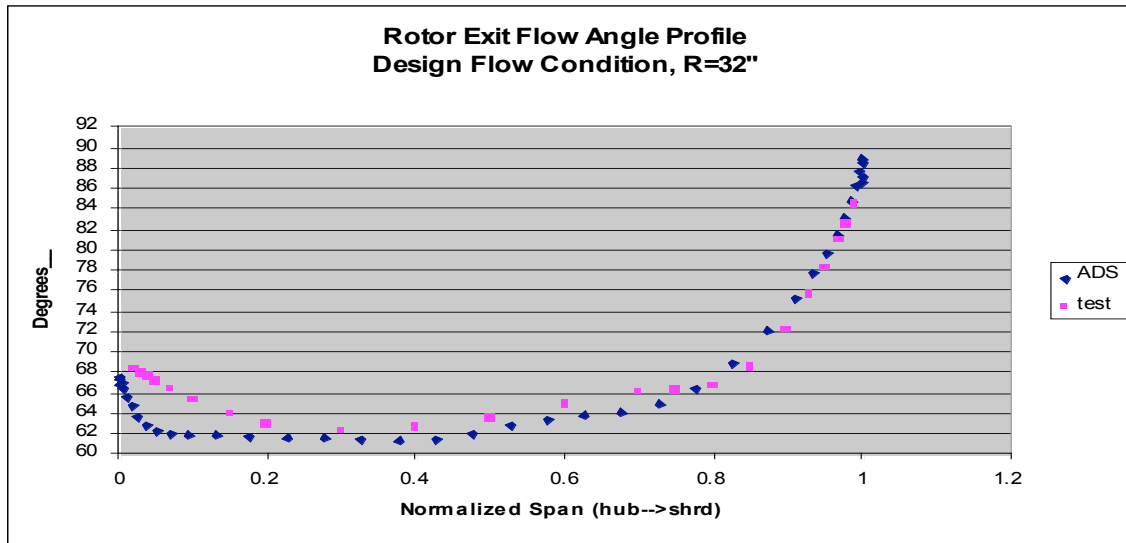


Figure 12, Rotor Total Pressure Ratio vs. Flow

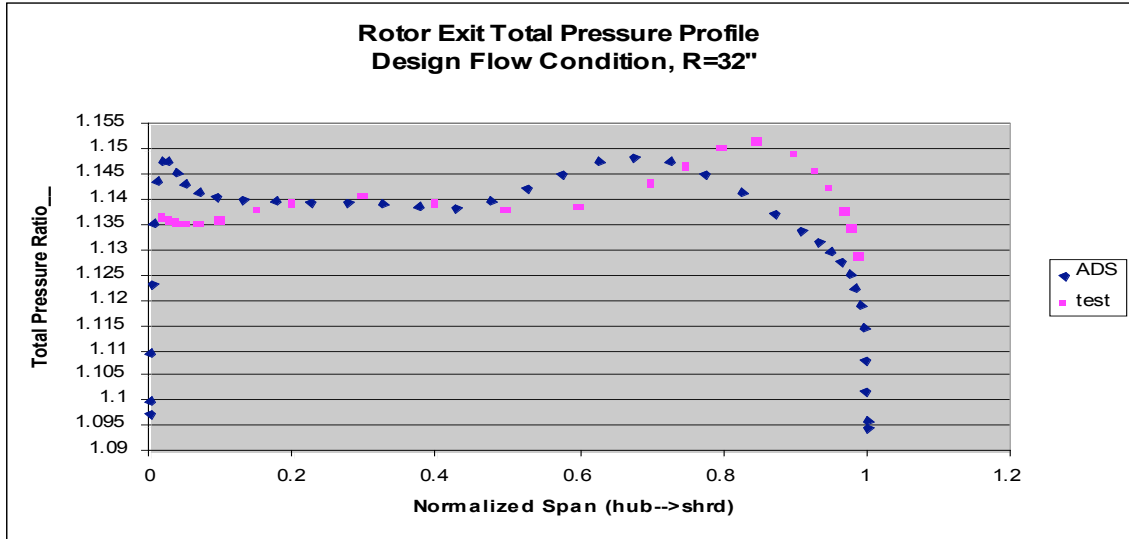


Figure 13, Rotor Total Pressure Ratio vs. Flow

Figures 14-16 are comparisons of CFD results against time-averaged laser anemometer data taken slightly downstream of the rotor trailing edge, at $R=30.42''$ ($r/r_2 = 1.014$). Relative tangential velocity normalized by rotor exit wheel speed is plotted from blade to blade at fixed spans.

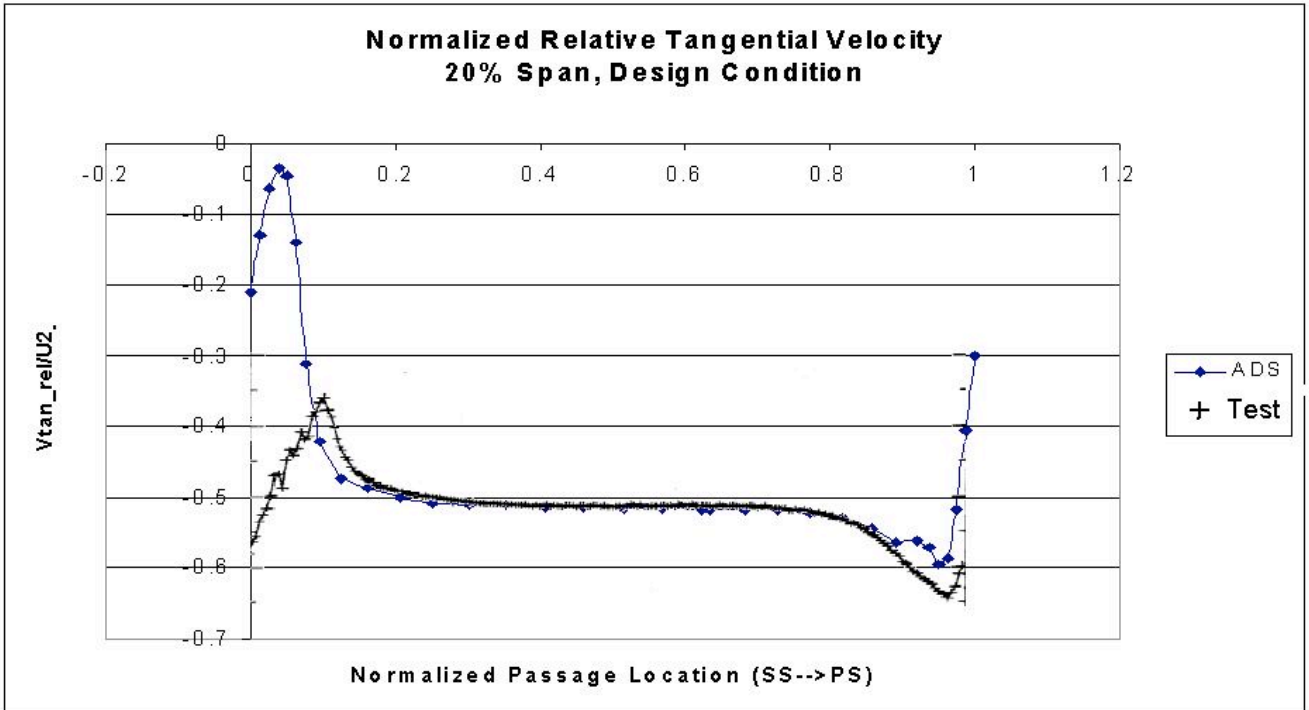


Figure 14, Blade-Blade Tangential Velocity Profile, Rotor Exit, 20% Span from Hub.

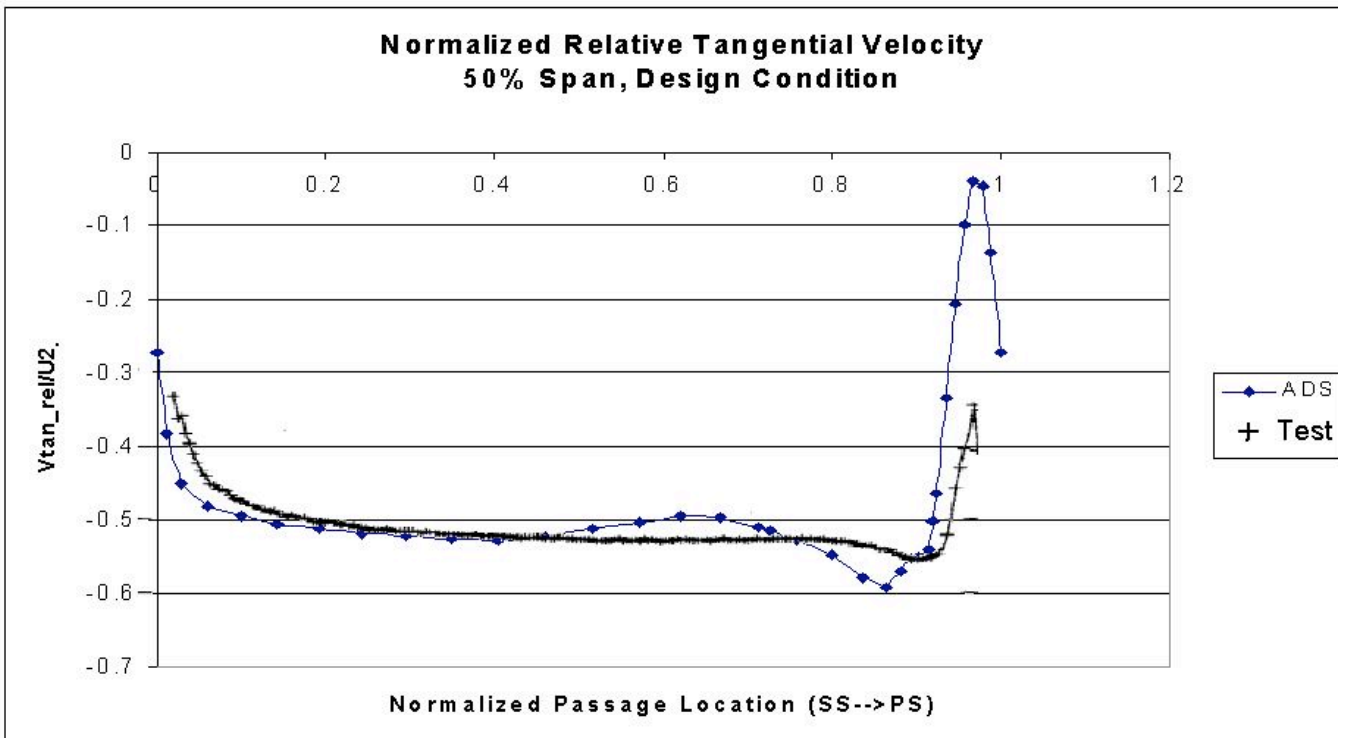


Figure 15, Blade-Blade Tangential Velocity Profile, Rotor Exit, 50% Span from Hub.

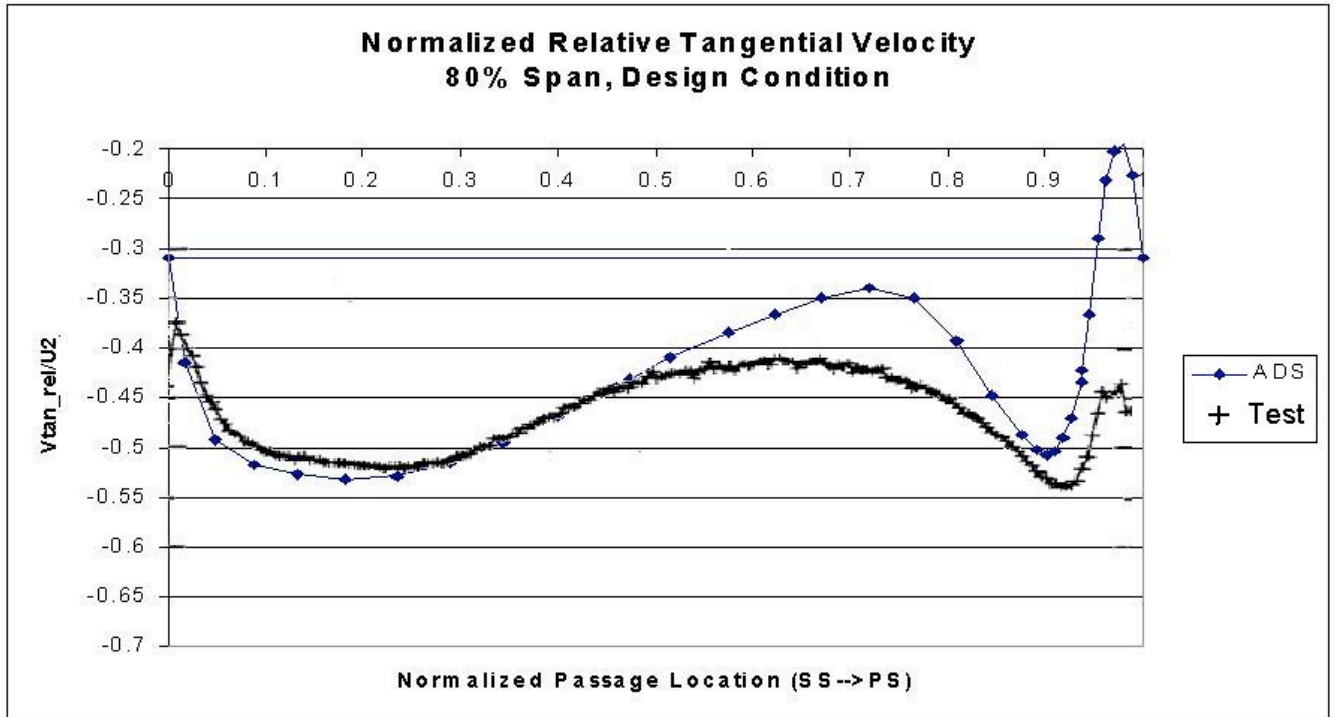


Figure 16, Blade-Blade Tangential Velocity Profile, Rotor Exit, 80% Span from Hub.

The above comparisons yield impressive correlation between CFD and test – particularly given the fact that the measurement station is so close to the rotor trailing edge. Not surprisingly, the comparison showing the greatest disparity is that near the shroud, where blade tip clearance and shroudline diffusion effects are prominent.

While it was intended to compare blade loading measurements and calculations, it was found that the static pressure test data reported were suspect and thus not used. The possibility of comparing blade loadings through blade surface velocity distributions was considered as an alternative approach. Unfortunately, the test data were not reported in a manner that facilitates a timely comparison of this type. Perhaps a closer look could be taken in the future.

G. References

- [1] Hathaway, M.,D., et. al., 1995, “Laser Anemometer Measurements of the Three-Dimensional Rotor Flow Field in the NASA Low-Speed Centrifugal Compressor,” Army Research Laboratory Technical Report, ARL-TR-333, June 1995.